

## High energy neutrino astronomy with Telescope Array detector

M. Sasaki<sup>1</sup>, Naohiro Manago<sup>1</sup>, and the other Telescope Array collaborators

<sup>1</sup>Institute for Cosmic Ray Research, University of Tokyo, Japan.

**Abstract.** We present the potential of the Telescope Array (TA) detector for deeply penetrating air-showers initiated by high energy neutrino from the most interesting source classes such as active galactic nuclei jets. The observation of high energy neutrino (HE- $\nu$ ) fluxes to correlate with these sources would be direct evidence for these objects to be the dominant sources of extremely high energy cosmic rays (EHECR). Adding to the highly-sensitive optical devices in the TA detector, the advanced frontend and trigger electronics fully utilizing high technology such as digital signal processor (DSP) will greatly contribute to maximizing the detection sensitivity irrelevant of air-shower kinematics. The TA detector, therefore, will probe astrophysical accelerators using good statistics of clearly identified neutrino-induced air-showers of the primary energy above  $10^7$  GeV with essentially no contaminations from protons and atmospheric neutrinos to lead opening the window of the HE- $\nu$  astronomy.

Spectrum Radio Quasars, while the rest are BL-Lac objects (Mattox et al., 1997). Blazars appear also to be able to explain about 25% of the diffuse extragalactic  $\gamma$ -ray emission (Mukherjee and Chiang, 1998). TeV  $\gamma$ -ray emission has been observed from blazars, the BL-Lac objects Mrk 421, Mrk 501, and 1ES2344+514 (Catanese, 1998). The data therefore strongly suggests that the highest energy photons originate in jets beamed to the observer (Punch et al., 1992) (Quinn et al., 1995) (Schubnell et al., 1996). Particles are expected to be accelerated by Fermi shocks in bunches of matter travelling along the jet with a bulk Lorentz factor of order  $\gamma \sim 10$ . Ultra-relativistic beaming with this Lorentz factor provides the natural interpretation of the observed superluminal speeds of radio structures in the jet (Rees, 1966) with the Doppler factor  $\Gamma$  of the same order as the Lorentz factor (Urry and Padovani, 1995).

Most theoretical work on  $\gamma$ -ray emission in AGN jets involved electron acceleration and inverse Compton scattering, and these models will predict no neutrinos. In electron blazar models the multi-wavelength spectrum consists of three components: synchrotron radiation produced by the electron beam on the magnetic field in the jet, synchrotron photons Compton scattered to high energy by the electron beam to produce the highest energy photons in the spectrum (Sikora Begelman and Rees, 1994). In order to reproduce the observed high energy luminosity, the accelerating bunches have to be positioned very close to the black hole. The same dense target will efficiently absorb the high energy photons by  $\gamma\gamma$  collisions. The natural cutoff therefore occurs in the 10-100 GeV region (Sikora Begelman and Rees, 1994). Finally, in order to prevent the electrons from losing too much energy before producing the high energy photons, the magnetic field in the jet has to be artificially adjusted to less than 10% of what is expected from equipartition with the radiation density.

In some of the proton blazar models energetic protons interact with radiation via pion photoproduction (Protheroe, 1996). Because of reduced energy loss, protons can produce the high energy radiation further from the black hole. The

---

### 1 Active Galactic Nuclei Neutrino

Active Galactic Nuclei (AGN) are a class of galaxies (Quasars, Blazars, Radio Galaxies, Seyferts, Optically Violent Variables, BL Lac's) which are characterized by large radio output and by large redshifts indicating not only extremely high power output:  $10^{42}$  to  $10^{48}$  erg/s but extremely compact (Jang and Miller, 1995). They are assumed to consist of a supermassive black hole, having as much as  $10^9$  solar masses surrounded by an accretion disk and a torus of hot gas. Jets are often seen along the axis of the disk. In a unified scheme of AGN, they correspond to Radio Loud AGN viewed from a position illuminated by the cone of a relativistic jet (Urry and Padovani, 1995). The 3rd EGRET catalog of high-energy  $\gamma$ -ray sources (Hartman et al., 1999) contains 66 high confidence identifications of AGN and 27 lower confidence potential ones. All belong to the blazar subclass, mostly Flat

---

Correspondence to: M. Sasaki  
(sasakim@icrr.u-tokyo.ac.jp)

favorable production-absorption balance makes it relatively easy to extend the high energy photon spectrum above 10 TeV energy, even with bulk Lorentz factors that are significantly smaller than in the inverse Compton models, describing the multi-wavelength spectrum of the AGN (Mannheim et al., 1996) (Protheroe, 1996). Because the density of photons is still much higher than that of target protons, the high energy cascade is initiated by the photoproduction of neutral pions by accelerated protons on ambient light via the  $\Delta$  resonance. The protons collide either with synchrotron photons produced by electrons (Mannheim et al., 1996), or with the photons radiated off the accretion disk (Protheroe, 1996). Model-independent evidence that AGN are indeed cosmic proton accelerators can be obtained by observing high energy neutrinos from the decay of charged pions, photoproduced on the  $\Delta$  resonance along with the neutral ones. The neutrino spectrum can now be calculated from the observed gamma ray luminosity. We recall that approximately equal amounts of energy are carried by the four leptons ( $e^+$ ,  $\nu_\mu$ ,  $\nu_e$ ,  $\bar{\nu}_\mu$ ) that result from the decay chain  $\pi^+ \rightarrow \nu_\mu \mu^+ \rightarrow e^+ \nu_e \bar{\nu}_\mu$ . The cross sections for the processes  $p\gamma \rightarrow p\pi^0$  and  $p\gamma \rightarrow n\pi^+$  at the  $\Delta$  resonance are the approximate ratio of 2 : 1. Thus a ratio of neutrino to  $\gamma$ -ray luminosities ( $L_\nu$ ,  $L_\gamma$ ) of approximately 1 : 3 neglecting pair-production process.

We assume that the target photon density spectrum is described by a  $E^{-1}$  power law and the number of target photons above photoproduction threshold grows when the proton energy is increased. For a standard non-relativistic shock, protons are accelerated to a power law spectrum with spectral index 2, the threshold effect implies that the spectral index of the secondary neutrino flux is also a power law with an index flattened by 1 as a result of the increase in target photons at resonance when the proton energy is increased. Therefore the normalization  $N$  can be obtained by:

$$\frac{dN_\nu}{dE_\nu} = N \cdot \left( \frac{E_\nu}{E_\nu^{Max}} \right)^{-1},$$

$$\int_{E_\nu}^{E_\nu^{Max}} dE_\nu E_\nu \frac{dN_\nu}{dE_\nu} \simeq N \cdot (E_\nu^{Max})^2 \simeq L_\nu \simeq \frac{L_\gamma}{3}.$$

In the case that the efficiency by which power in the shock is converted into acceleration of particles reach values close to 1, the maximum proton energy reaches:  $E_p^{Max} = eBRc = 5 \times 10^{19}$  eV for  $B \sim 5$  Gauss and  $R \sim 0.02$  parsecs. The average energy carried by the neutrino in the photoproduction and decay chain, is roughly 1/20 of the parent proton energy. Finally the maximum neutrino energy is estimated to be  $E_\nu^{Max} = \frac{1}{20} E_p^{Max} \sim 10^{18}$  eV.

In some proton blazar models (Halzen and Zas, 1997), only interactions of protons with radiation via pion photoproduction ( $p\gamma$ ) would lead to neutrino production as described above. The other models (Protheroe, 1996) (Stecker and Salamon, 1995) (Szabo and Protheroe, 1992) (Mannheim, 1995) count contributions both from the processes of ( $p\gamma$ ) and ( $pp$ ) which makes a significant change of the spectrum in the lower energy region below  $10^{15}$  eV. Diffuse neutrino flux

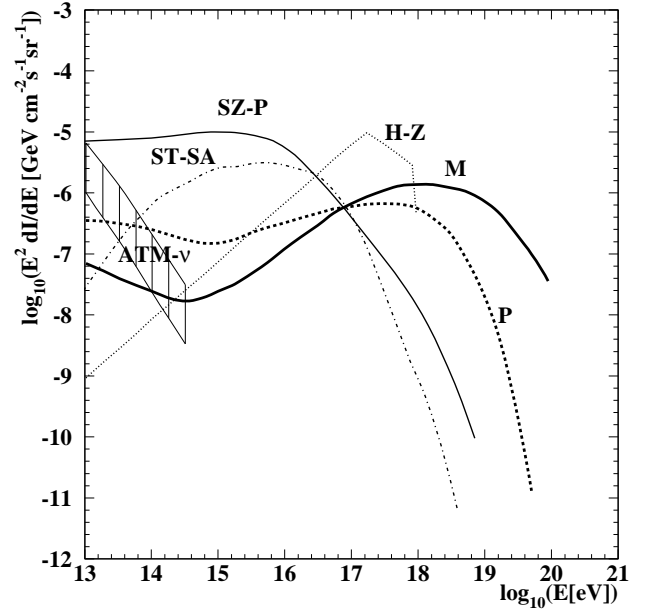


Fig. 1. Diffused neutrino flux from AGN (See text).

predictions assuming the neutrino productions in the cores and in the jets are illustrated in Fig.1 assuming Blazars appear to be able to explain about 25% of the diffuse  $\gamma$ -ray emission and the electron and muon neutrinos contribute to the flux but approximately the electron neutrino flux is a factor of two below the muon neutrino for all cases. In Fig.1, the range of atmospheric neutrino background as the zenith angle changes from  $0^\circ$  to  $90^\circ$  (Lipari, 1993), which appears to have so large spectral index that it cannot largely contribute to neutrino detection in the higher energy region above  $10^{15}$  eV in any proton blazar models.

## 2 Detection of Active Galactic Nuclei Neutrino

The TA detector has been designed in order to clarify the mystery of the origin of the highest energy cosmic rays (Sasaki, 1997) (TA Design Report, 2000). The TA detector consists of 10 observational stations installed on the line in about 30-40km interval in the Utah south. Each station consists of 40 telescopes with 3m-diameter  $f/1$  mirror system on 2 layers of supports. 256 2-in PMTs mounted on the focal plane are served as pixels of the fluorescence sensor of each telescope. Each PMT covers the visual field which makes 1.2 degrees to be angular aperture. It is expected to provide excellent particle identification as well as accurate directional determination of primary cosmic rays to test the source models at a high confidence level. by imaging fluorescence yielded in air-showers reconstructing the longitudinal development with a huge effective aperture.

We consider both deep inelastic charged and neutral current interactions which always produce hadronic showers. In the case of charged current electron neutrino interactions the

emerging electron contributes in addition a pure electromagnetic shower carrying a large fraction of the incoming particle energy. For a neutrino flux  $dI_\nu/dE_\nu$  interacting through a process with differential cross section  $d\sigma/dy$ , where  $y$  is the fraction of the incident particle energy transferred to the target, the event rate for deeply penetrating showers can be obtained by a simple convolution:

$$\text{Rate}[E_{sh} > E_{th}] =$$

$$N_A \rho_{air} \int_{E_{th}}^{\infty} dE_{sh} \int_0^1 dy \frac{dI_\nu}{dE_\nu}(E_\nu) \frac{d\sigma}{dy}(E_\nu, y) \epsilon(E_{sh}),$$

where  $N_A$  is Avogadro's number and  $\rho_{air}$  is the air density. The energy integral corresponds to the shower energy  $E_{sh}$  which is related to the primary neutrino energy  $E_\nu$  in a different way depending on the interaction being considered.  $\epsilon$  is a detector acceptance, a function of shower energy, which corresponds to the volume and solid angle integrals for different shower positions and orientations with respect to the detector. The function is different for showers induced by charged current electron neutrino interactions from those arising in neutral current or muon neutrino interactions. This is because hadronic and electromagnetic showers have differences in the particle distributions functions, particularly for muons. For  $(\nu_e + \bar{\nu}_e)N$  charged current interactions, we take the shower energy to be the sum of hadronic and electromagnetic energies,  $E_{sh} = E_\nu$ . For  $(\nu_\mu + \bar{\nu}_\mu)N$  charged current interactions and for neutral current interactions, we take the shower energy to be the hadronic energy,  $E_{sh} = yE_\nu$ . For the moment, we don't take into account any type of neutrino oscillation during the propagation from AGN to the earth. Adding that, to simplify the event rate evaluations, here we neglect the distribution of  $\frac{d\sigma}{dy}(E_\nu, y)$  as a function of  $y$  replacing it into  $\frac{d\sigma}{dy}(E_\nu, y = 0.2)\delta(y - 0.2)$  in Eq.2 because  $\langle y \rangle \sim 0.2$  does not depend on the primary energy beyond  $10^{16}$  eV in both cases of charged and neutral current interactions (Gandhi et al., 1995). We use new calculations of the cross sections for charged-current and neutral current interactions of neutrinos with nucleons (Gandhi et al., 1995), according to the CTEQ4-DIS (deep inelastic scattering) parton distributions (CTEQ, 1997).

For our event rate calculation we select the prediction of (Szabo and Protheroe, 1992), labelled SZ-P. Most recent models for the proton blazars site the acceleration in the jets themselves. We use the prediction of (Mannheim, 1995), labelled M, which illustrates that the emitted neutrinos may extend well into the EeV region.

Each simulation for a given primary cosmic ray (electron neutrino, muon neutrino, or proton) was performed at fixed energy. The shower energy of neutrinos depends on the generation as described above. In the simulation we fix the energy transfer parameter  $y$  to be the average value  $\langle y \rangle = 0.2$ , which is reasonable for  $E_\nu > 10^{16}$  eV. For each shower energy, the mean depth of proton shower maximum was determined from simulations. For each primary particle at each energy, the mean of the interaction length  $X_1$  was determined

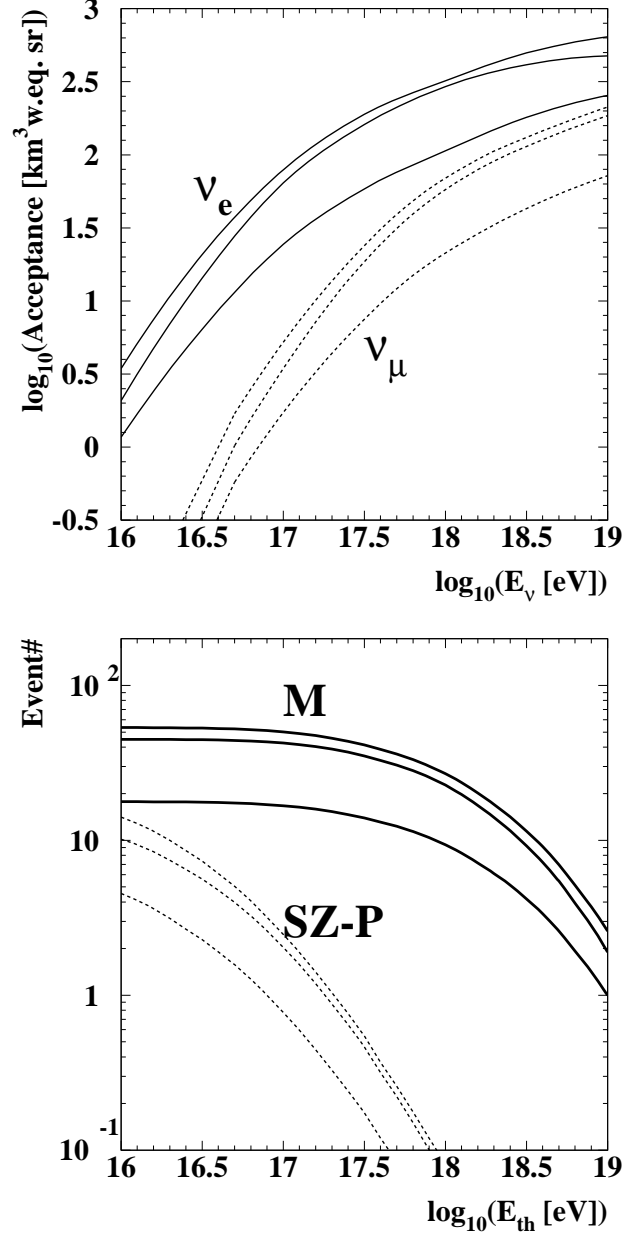


**Fig. 2.** *Left:* Acceptance of the TA detector to neutrino induced air shower. Volume units are km<sup>3</sup> of water equivalent. *Right:* Annual event rates as a function of the neutrino energies in the TA detector for neutrino induced air showers with fluxes from two different AGN models (see text). The higher, middle, and lower curves corresponds to events after preselection, track quality, and proton rejection cuts.

from the above interaction cross sections of neutrinos with nucleons or that of protons,  $83.1(E/GeV)^{-0.052} \text{g/cm}^2$  (Honda et al., 1993). The shower energy determines the shower size at maximum,  $N_{max}$  (Baltrusitis et al., 1985). Given  $N_{max}$ ,  $X_{max}$ , and  $X_1$ , the complete longitudinal profile was described by the Gaisser-Hillas function (Gaisser and Hillas, 1977). The NKG lateral distribution function (Kamata, Ni-

shimura, Greisen, 1958,1956) normalized with the Gaisser parametrization has been used for the total number of electrons and positrons in hadronic (electromagnetic) cascade showers to determine the location where fluorescence lights are produced. We took into account the fluctuations of the first interaction depth, impact point, and directional angles of air shower cores with appropriate distributions but not air shower size fluctuations. The light yield arriving at the detector site is calculated. Rayleigh and Mie scattering processes are simulated, with full account taken of the spectral characteristics of the light. The isotropically emitted fluorescence light, is propagated, while we have not implemented direct and scattered Cerenkov light yet. Night sky background noise is added to the signal. All processes that affect to overall optical efficiency; mirror area and reflectivity, optical filter transmission, PMT quantum efficiency factors are folded with the light spectrum to give the photoelectron yield in each PMT, due to signal and noise. A "fired" PMT is defined to require that its instantaneous photoelectron current is greater than the  $2.5\sigma$  noise level of the night sky background. We preselected events if at least one of 10 eyes contains at least 10 firing PMTs. To ensure track quality, we cut events of which shower maximums are not viewed by any eye. Finally to reject proton background events, we selected only events with  $X_{max} > 1300 \text{ g/cm}^2$ . We obtained the detector apertures corresponding the above selection cuts and calculated them into the acceptances multiplying the appropriate interaction length of neutrino with nucleon. The results are shown in Fig.2 for both electron and muon neutrinos as a function of the primary energy. The results of the TA acceptance and event rates are shown in Fig.2. Annually more than ten AGN neutrinos will be identified by TA in the case of (Mannheim, 1995) against no intrinsic atmospheric neutrino background, assuming overall duty factor to be 10%.

The TA detector ultimately will probe extraterrestrial accelerator sources using enough statistics of clearly identified neutrinos. Also we can distinguish between the assumptions for the location in AGN where protons could be accelerated

from the observed spectrum above the energy of  $10^{16} \text{ eV}$ .

## References

- M.Jang and H.R.Miller, *Ap.J.*, **452** (1995) 582.  
 C.M.Urry and P.Padovani, *Pub. Astr. Soc. Pacif.*, **107** (1995) 803.  
 R.C.Hartman, et al., *Ap. J. Suppl.*, **123** (1999) 79.  
 J.R.Mattox et al., *Ap. J.*, **438** (1997).  
 R.Mukherjee and J.Chiang, astro-ph/9902003. J.Chiang and R.Mukherjee, *Ap. J.*, **496** (1998) 752.  
 M.Catanese, *Ap. J.*, **501** (1998) 616.  
 M.Punch et al., *Nature*, **358** (1992) 477.  
 J.Quinn et al., *Ap. J.*, **456** (1995) L83.  
 Schubnell et al., astro-ph/9602068.  
 M.J.Rees, *Nature*, **211** (1966) 468.  
 M.Sikora, M.C.Begelman, and M.J.Rees, *Ap. J. Lett.*, **421** (1994) 153.  
 R.J.Protheroe, astro-ph/9612213.  
 K.Mannheim, et al., astro-ph/9605107.  
 R.J.Protheroe, ADP-AT-96-4.  
 F.Halzen and E.Zas, MADPH-97-982, astro-ph/9702193.  
 F.W.Stecker and M.H.Salamon, astro-ph/9501064.  
 A.P.Szabo and R.J.Protheroe, Proc. High Energy Neutrino Astrophysics Workshop (U.Hawaii, March 1992), ed. V.J.Stenger, J.L.Learned, S.Pakvasa, and X.Tata, World Scientific, 1993, p24.  
 K.Mannheim, *Astrop. Phys.* **3** (1995) 295.  
 P.Lipari, *Astrop. Phys.*, **1** (1993) 195.  
 M. Sasaki et al., Proc. 25th ICRC, **5**, 369 (Durban, 1997).  
 The Telescope Array Project: Design Report. July 2000. <http://www-ta.icrr.u-tokyo.ac.jp>  
 R.Gandhi, C.Quigg, M.H.Reno, and I.Sarcevic, *Astrop. Phys.*, **5** (1995) 81. R.Gandhi, C.Quigg, M.H.Reno, and I.Sarcevic, *Phys. Rev.*, **D58** (1998) 093009.  
 T.K.Gaisser and A.M.Hillas, *Proc.15th Int.Conf.Cosmic Rays, Plovdiv,Bulgaria*, **8** (1977) 353.  
 CTEQ Collaboration, H.L.Lai et al., *Phys. Rev.*, **D55** (1997) 1280.  
 M.Honda et al., *Phys. Rev. Lett.*, **70** (1993) 525.  
 R.M.Baltrusitis et al., *Proc. 19th ICRC, La Jolla*, **7** (1985) 159.  
 K.Kamata and J.Nishimura, *Prog. Theor. Phys. Suppl.*, **6** (1958) 93.  
 K.Greisen, *Prog. Cosmic Ray Physics*, **3** (1956) 1.